Organic & Biomolecular Chemistry

PAPER

View Article Online
View Journal | View Issue

Cite this: *Org. Biomol. Chem.*, 2014, **12**, 5621

Elucidating factors leading to acidolytic degradation of sterically strained oligoether dendrons†

J. Karabline-Kuks, A. Fallek and M. Portnoy*

Received 11th March 2014,
Accepted 30th May 2014

DOI: 10.1039/c4ob00540f

www.rsc.org/obc

While steric hindrance can be particularly large in dendritic molecules, it is usually implicated with difficulties in the synthesis of higher generation structures and restricted access of reagents, including bond-cleaving agents, to the dendritic interior. A different situation, where the steric hindrance is translated into a steric strain within the dendritic molecule and, consequently, causes enhanced decomposition of the dendron-containing structure, has only occasionally been reported and exclusively for dendronized polymers. In this work we describe post-synthetic cleavage of sterically congested third-generation oligoether dendrons from solid supports, followed by their disassembly into monomeric building blocks under acidic conditions. This disassembly was monitored by H NMR, revealing the intermediate fragment structures and the exact order of bond cleavage within the dendritic molecule. These conclusions were supported by MS analysis of the cleavage mixtures. Though distinguishing between steric and electronic reasons of molecular disassembly can be a challenging task, we were able to analyze these factors separately by monitoring the dendron disassembly and comparing the rates of "decay" of parent dendrons and their fragments. This comparison reveals that while the electron donation of the steric congestion-inducing alkyl substituents is a prerequisite for the disassembly of the structures, this disassembly is very strongly accelerated in the sterically crowded dendrons and intermediates, where both steric and electronic factors contribute in a synergistic way to the disassembly phenomenon.

Introduction

Steric crowding induces steric strain in certain organic molecules and, accordingly, can lead to the increased propensity of these molecules to undergo decomposition.[1] Frequently, the substituents that induce steric congestion also have an electronic influence, and hence the cause of decomposition can also be attributed to electronic factors. Therefore, distinguishing between steric and electronic reasons of molecular disassembly could become a challenging task.

Steric hindrance can be particularly large in dendritic molecules and macromolecules, due to their highly branched nature.[2] This hindrance is known to preclude synthesis of larger dendritic structures or, *vice versa*, to inhibit disassembly of degradable dendritic molecules by obstructing access of reagents to the built-in labile functionalities.[3,4] On the other hand, there are very few examples of the disassembly of dendritic structures facilitated by steric strain.[5] Moreover, to the best of our knowledge, these few examples were reported for dendronized polymers, rather than for isolated dendrimers or dendrons. Due to the numerous proposed uses of dendrimers with sterically-demanding groups,[6] it is of considerable importance to understand the limitations of sterically crowded dendritic molecules, particularly with regard to their stability.

We have recently reported that sterically crowded polyether dendrons can be prepared on a solid polystyrene support up to the third generation (Fig. 1a).[7–9] We also observed and reported that upon exposure to acid these structures undergo a facilitated disassembly (as compared to their analogues that lack strain-inducing substituents). Using model "hetero-dendrons" prepared from both the sterically congested and strain-free monomers (Fig. 1b,c), we demonstrated that it is primarily the electronic influence of the substituents (stabilization of the benzylic cations by the *ortho*- and *para*-positioned propyls) that leads to the diminished stability of the dendrons. However, the differences in the decomposition rates of the "homo-" and "hetero-dendrons" pointed to an additional factor that may be electronic (the increase in the basicity of the phenol oxygen) or steric. In addition, substantial differences

School of Chemistry, Raymond and Beverly Sackler Faculty of Exact Sciences, Tel Aviv University, Tel Aviv 69978, Israel. E-mail: portnoy@post.tau.ac.il

†Electronic supplementary information (ESI) available: Spectra of the H NMR monitoring of the acidolytic disassembly of the dendrons **G3(E)** and **G3des$_{1,3}$(E)**, the synthesis of **G3des$_{1,3}$(E)**, as well as the relevant MS spectra. See DOI: 10.1039/c4ob00540f

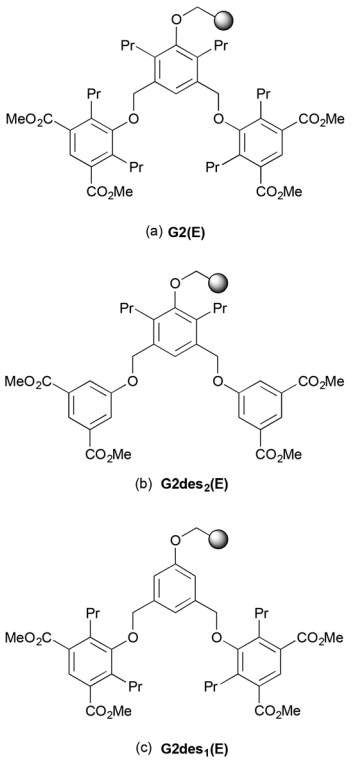

Fig. 1 Second-generation "homo-" and "hetero-dendrons".[7]

were observed in the decomposition rates of the dendrons *vs.* their partially-disassembled successors, clearly pointing to the involvement of the steric strain. In order to further explore the observed phenomenon and, possibly, elucidate all the factors leading to the acid-induced disassembly of the dendrons, we decided to carefully monitor the decomposition of the third-generation structures: the previously reported "homo-dendron", as well as a "hetero-dendron" especially prepared for these experiments. We herein report the results of this study. This investigation could shed light on the stability of oligoether dendrons in a low pH environment, with implications on their potential use in drug delivery systems and other biomedical devices.

Results and discussion

Following its cleavage from the support, the third-generation dendron **G3(E)** can disintegrate into monomeric building blocks by a number of parallel or intersecting routes, schematically depicted in Scheme 1. If all of them occur in parallel with the same probability during the NMR monitoring of the acidolytic disassembly of the dendron, one may expect a series of very complex spectra, which will be practically impossible to decipher. Fortunately, monitoring of the dendron decomposition in a 9 : 1 $CDCl_3$–TFA mixture (Fig. 2) exhibited the formation of 6 to 7 major fragments only (Fig. 3), in such a way that their formation from the third-generation dendron or interconversion can be followed with reasonable ease and a degree of confidence.

The identification of various species in the reaction mixture was based primarily on the aromatic proton signals and the signals of protons in *O*-substituted benzylic positions. The assignment of the signals was based on chemical shifts, expected when taking into account electronic and steric influence of the neighbour substituents, as well as the general NMR data and the NMR data specific to the related dendritic molecules.[7–9,11] In addition, we based the assignment of the signals on their size and their size changes during the monitoring. The position of the aromatic protons of the various dendrons and fragments is highly sensitive to the *ortho* and *para* substituents, as well as to the steric crowding around them. Thus, the combined electron-withdrawing effect of two *ortho* carbomethoxy groups induces a strong downfield shift of the aromatic proton signal (appearing at 7.92 to 8.14 ppm), as compared with the protons neighbouring two oxyalkyl groups (the "inner" modules of dendrons and fragments). The position of the aromatic protons is also influenced by the *para* substituent, with the hydroxy group (focal point modules and the **G1(E)** building block) affecting an upfield shift of the proton signal, as compared to the position of those with a benzyloxy substituent. Finally, the steric crowding can substantially shift downfield the position of aromatic protons, compared to the position of protons with similar *ortho* and *para* substituents. In other words, the "deeper" inside the dendritic structure is located a given proton, the more downfield its signal will appear, when compared to its analogue positioned closer to the periphery. A similar trend was observed previously for various aryl–benzyl ether dendrons.[9,11] In the spectral area characteristic to protons of *O*-substituted benzylic methylenes, chemical shifts in the 4.86–5.00 ppm range were characteristic to benzyl ethers, while those in the range of 5.38–5.45 ppm were characteristic to benzyl trifluoroacetate esters.

Notably, the **G3(E)** dendron appears as a main component of the mixture in the first spectra of the monitoring sequence and exhibits characteristic aromatic (8.136, 7.803 and 7.708 ppm) and low-field benzylic signals (4.995 and 4.925).[12] It is important to mention that, according to the first spectra of the series, the third-generation dendron was slightly contaminated by lower generation dendrons (**G2(E)** and **G1(E)**). However, since these species are also part of the disassembly chain of **G3(E)** (as we will show subsequently), these impurities did not complicate the analysis of the decomposition pattern.

The first spectra of the sequences clearly show two major fragments being created from **G3(E)**, nearly in parallel. The first was identified capitalizing on a prior art as **G2(E)**, which exhibits characteristic aromatic (8.128 and 7.520 ppm) and a low-field benzylic (4.893 ppm) signals.[7] The second fragment exhibited distinct aromatic singlets at 8.141 and 7.339 ppm and distinct benzylic singlets at 5.436 and 4.943 ppm. Two additional singlet signals of this fragment, an aromatic and a benzylic, at 7.797 and 4.922 ppm respectively, were concealed in these spectra by the closely situated signals of **G3(E)**, but

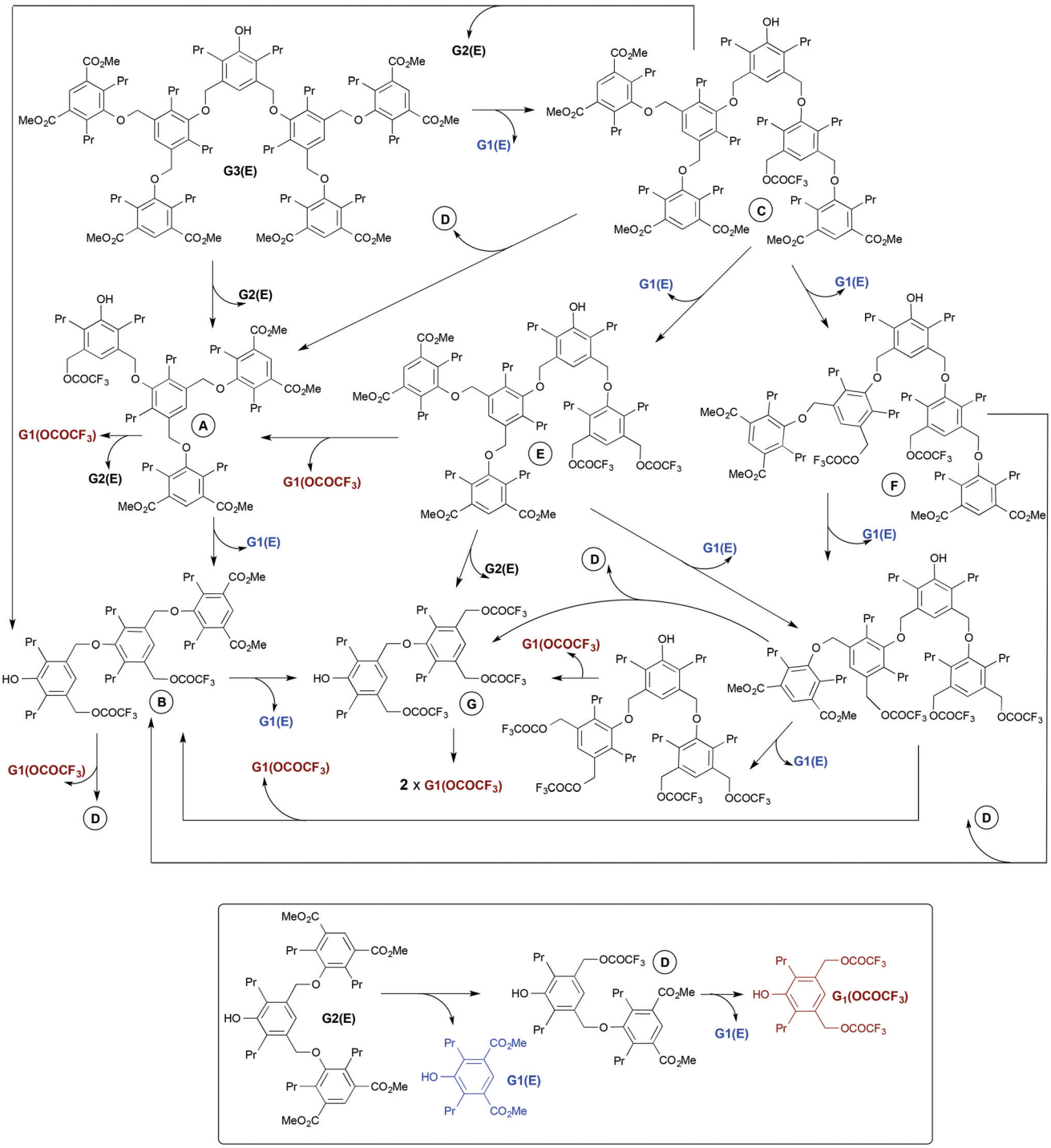

Scheme 1 All possible routes for the disassembly of **G3(E)**.

became clearly visible in the later spectra of the series. This set of signals was attributed to fragment **A** (Fig. 3). Concurrent growth of the **G2(E)** portion in the cleavage mixture supports this assignment, since cleavage of **G2(E)** from **G3(E)** will inevitably lead to the formation of **A**.

Subsequent spectra of the decomposition monitoring reveal the expected disassembly of the **G2(E)** dendron to **G1(E)** and fragment **D**, according to our past observations.[7] **G1(E)** is characterized by the characteristic aromatic singlet at 7.924 ppm, while compound **D** exhibits a distinct aromatic signal at 7.241 ppm and distinct low-field benzylic signals at 5.416 and 4.858 ppm. In addition, one of the aromatic signals of **D** at 8.129 ppm merges with the signal of **G2(E)** at the same location.

The fate of fragment **D**, known from our previous study, is the disassembly into another equivalent of **G1(E)** and a reduced first-generation module **G1(OCOCF$_3$)**. Indeed, in the

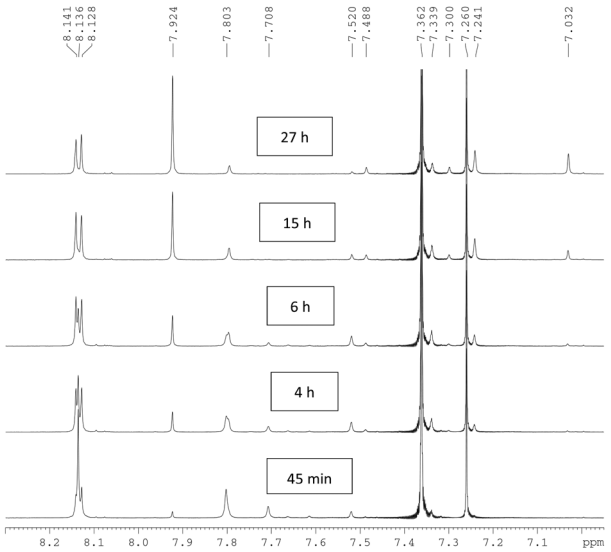

Fig. 2 H NMR monitoring of the disassembly of **G3(E)** in a 9 : 1 $CDCl_3$–TFA mixture.[10] Residual $CHCl_3$ and benzene reference appear at 7.260 and 7.362 ppm, respectively.

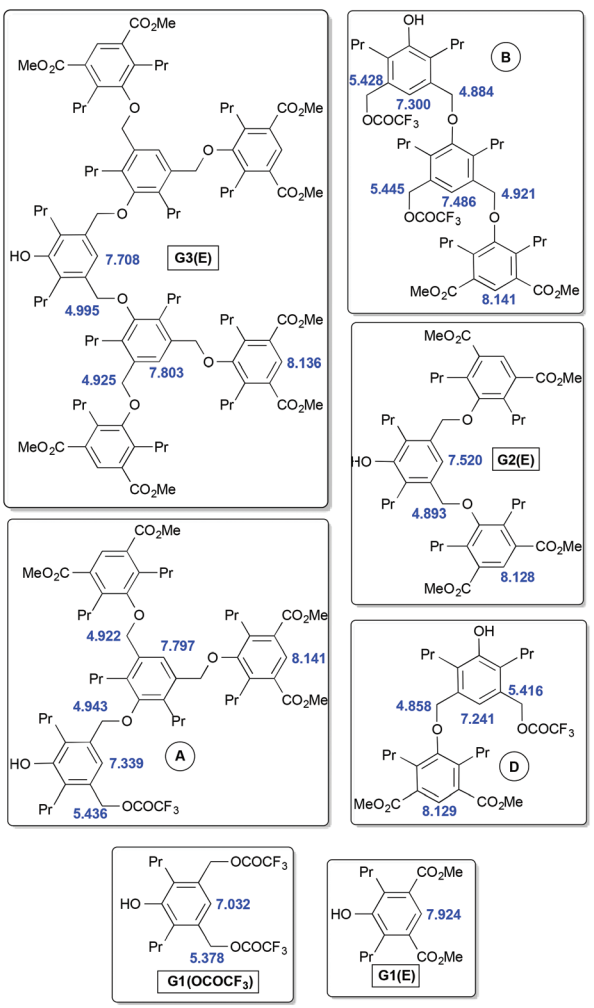

Fig. 3 Dendrons and fragments, observable in a 9 : 1 $CDCl_3$–TFA mixture, and their characteristic chemical shifts.

later spectra of the monitoring series, an aromatic signal at 7.032 ppm and a benzylic signal at 5.378 ppm, gradually increasing in intensity, are attributed to the **G1(OCOCF$_3$)** fragment.

The mode of disassembly of the fragment **A** is more difficult to track. While it can disintegrate into **G2(E)** and **G1(OCOCF$_3$)**, we cannot be sure what the contribution of this mode of decomposition to the disassembly of **A** is, since both fragments are generated by alternative routes. An additional mode of the disintegration of **A** leads to **G1(E)** and a fragment **B** (Fig. 1). While **G1(E)** is also formed in a number of the above mentioned fragmentations (disassembly of **G2(E)** and of **D**), the generation of **B** in the cleavage solution is likely to proceed mostly through this route (*vide infra*) and will constitute a proof for the existence of this mode of decomposition of **A**. Beginning a few hours from the start of the cleavage and disassembly, a new set of signals gradually appears (in the earlier spectra most of the signals are concealed by the larger signals of other fragments) and becomes distinct in the later monitoring spectra. The set includes the aromatic singlets at 8.141, 7.486 and 7.300 ppm as well as the low-field benzylic singlets at 5.445, 5.428, 4.884 and 4.921 ppm. Such a set of signals best fits the proposed fragment **B**. Moreover, the decline in the amount of **A**, which begins after 11 hours of the monitoring, is largely compensated by the increase in the amount of the fragment responsible for the appearance of these peaks. This observations postulates that **B** is indeed formed, and the conversion of **A** into **B** and **G1(E)** is the preferred mode of **A**'s disassembly.

All the fragments observed in the cleavage mixture and described above can be explained by the primary disassembly event of **G3(E)** breaking into **A** and **G2(E)**. This, however, leaves open the question whether another mode of **G3(E)** decomposition, breakage into **G1(E)** and a fragment **C**, actually takes place during the acidolytic disassembly (Scheme 1). Having a very similar structure to **G3(E)**, fragment **C** is likely to exhibit NMR signals that are very similar to those of its parent compound. Thus, if **C** is produced, most of its signals will be concealed by those of **G3(E)**. However, the aromatic and benzylic signals, closest to the site of cleavage that formed this fragment, must be very different from those of its parent structure. We expect that the chemical shifts of these two signals will be similar to those of the related hydrogens in **B**, *i.e.* 7.486 and 5.445 respectively. Since **B** accumulates in the solution in a detectable amount only after a few hours (*ca.* 4 h), while the hypothetical fragment **C** must be formed (if at all) during the initial stages of the monitoring whilst the concentration of **G3(E)** is the highest, there is a time window when the two distinct signals of **C** can be detected. A careful examination of the first spectra of the monitoring series indeed reveals two very small signals at 7.489 and 5.446 ppm, which cannot be attributed to **B**, since other characteristic signals of **B** are still missing in these spectra. Once the presence of **B** becomes visible, these two signals merge with the related signals of **B**, until *ca.* 11 h from the start of monitoring the presumable signals of **C** are not detectable any more.

Even if we accept the assumption that the signals at 7.489 and 5.446 ppm represent **C**, its amount during the monitoring, particularly at the early stages when it is supposed to be the highest, is negligible. Moreover, during these early stages of the disassembly, the potential products of its four possible decomposition modes are either present in negligible amounts (**D** and **B**, Scheme 1), or are not detected at all (**E** and **F**, Scheme 1). The latter observation rules out the possibility of slow formation/fast decomposition of **C** and, together with the first observation, proves that the main route of decomposition of **G3(E)** proceeds through **A** and **G2(E)**, while the pathway proceeding through **C** and **G1(E)** is very minor at most.

The last point to address, in regard to the NMR monitoring, is the fate of **B**. Though it can decompose to a hypothetical fragment **G** and **G1(E)**, no evidence for **G** was found in the latest spectra of the monitoring series, when the concentration of **B** in the mixture was the highest. Thus, it is logical to assume that **B** mainly decomposes to **G1(OCOCF$_3$)** and **D**.

Based on the above analysis of the NMR monitoring of the acidolytic disassembly of the third-generation dendron, **G3(E)**, we can reconstruct the actual disassembly route that is depicted in Scheme 2. Some of the pathways seem very reasonable (**A** to **G1(OCOCF$_3$)** + **G2(E)**, **B** to **G1(OCOCF$_3$)** + **D**) but could not be verified since their products are also formed by competing pathways. The "detour" *via* **C** is a minor pathway at most, and it is also not clear if **C** decays to **B** + **G2(E)** or to **A** + **D**, since all these fragments are formed *via* competing processes of the main decomposition "chain".

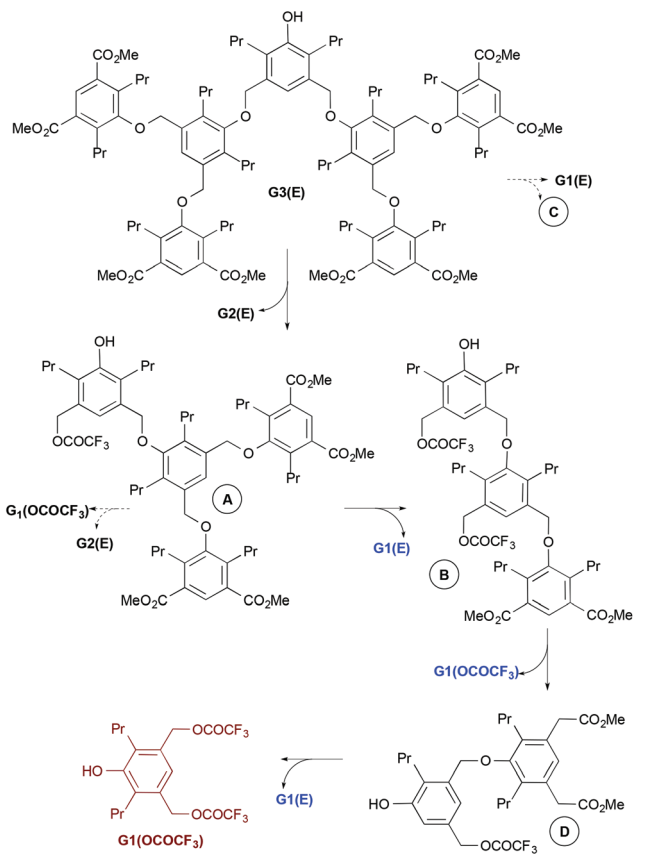

Scheme 2 The actual disassembly route of **G3(E)**.

The proposed disassembly route was confirmed also by two ES-MS analyses of the mixture composition. In both positive and negative peak detection modes, the measurement carried out *ca.* 45 minutes after the beginning of the cleavage exhibited the characteristic $(M + Na)^+$ and $(M + CF_3CO_2)^-$ peaks of **G3(E)** (*m*/*z* 1807.3 and 1897.0 respectively), as well as those of **A** (*m*/*z* 1129.7 and 1219.5 respectively) and **G2(E)** (*m*/*z* 813.5 and 903.4 respectively). Smaller peaks that can be attributed to **B** (*m*/*z* 949.4 and 1039.4 in the positive and negative ion detection modes respectively) and **D** (*m*/*z* 633.2 in the positive mode only) were also observed.[13] Small signals at *m*/*z* 1626.8 and 1716.8, in the positive and negative detection modes respectively, can be considered as an evidence for the presence of a trace amount of **C** and, hence, as an additional proof of the minor pathway involving this fragment. In both detection modes there are no peaks that can be attributed to any other fragment depicted in Scheme 1.[14] The measurement carried out after the mixture was incubated for 27 hours demonstrated a complete disappearance of **G3(E)** and **C**, along with a notable decrease in the intensity of the signals of **G2(E)**, while the signals of **A** remained strong. This change was accompanied by a significant increase in the intensity of the signals attributed to **B** and **D**. Due to the high abundance of **G1(E)** and **G1(OCOCF$_3$)** in the mixture, their $(M - H)^-$ peaks are clearly visible in the negative ion detection mode (*m*/*z* 293.1 and 429.1 respectively), in spite of the low molecular mass of these fragments. Very weak peaks in the positive and negative detection modes may point to trace amounts of **E**/**F** (*m*/*z* 1445.7 and 1535.7 for the $(M + Na)^+$ and $(M + CF_3CO_2)^-$ peaks respectively). A low intensity signal in the positive mode (*m*/*z* 769.3 for the $(M + Na)^+$ peak) and a stronger signal in the negative mode (*m*/*z* 859.3 for the $(M + CF_3CO_2)^-$ peak) may point to the presence of fragment **G** in the mixture. This evidence, however, is not supported by the NMR findings.

Additional information shedding light on the factors responsible for the degradation of this type of dendrons was obtained from monitoring the decomposition of the mixed dendron **G3des$_{1,3}$(E)** (Scheme 3),[15] which was prepared by a route similar to that applied for other dendrons using the simpler dimethyl 5-hydroxyisophthalate building block, instead of its dipropylated analogue, for the assembly of the first and third layers. It is important to mention that, according to the first spectra of the monitoring series, the dendron **G3des$_{1,3}$(E)** was slightly contaminated by lower generation dendrons (**G1des(E)** and **G2des$_2$(E)**). However, since the first of these impurities is a part of the disassembly chain of **G3des$_{1,3}$(E)** (as we will show below), while the second decomposes quickly (within 1 day) into known fragments according to the pathway described by us previously,[7] these impurities did not complicate the analysis of the decomposition pattern.

It is noteworthy that **G3des$_{1,3}$(E)** is practically stable in a 9 : 1 $CDCl_3$–TFA mixture, which led to complete decomposition of **G3(E)** within 11 hours. H NMR follow-up of the decomposition of **G3des$_{1,3}$(E)** in a 1 : 1 $CDCl_3$–TFA cleavage solution

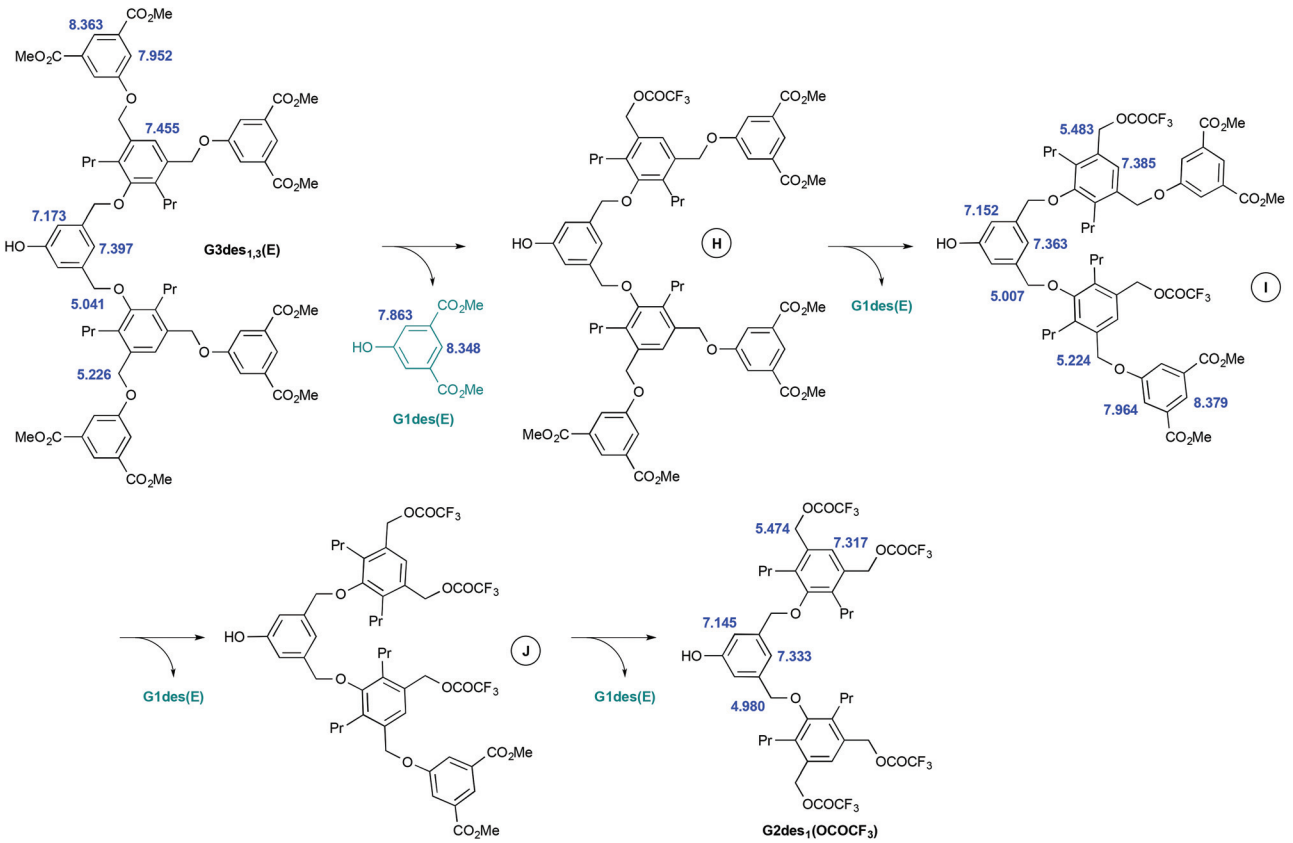

Scheme 3 The disassembly route of **G3des$_{1,3}$(E)** and the characteristic chemical shifts of the dendron and the fragments.

exhibited the slow conversion of the parent dendron, characterized by aromatic signals (8.363(t), 7.952(d), 7.455, 7.397 and 7.173 ppm) and low-field benzylic signals (5.226 and 5.041 ppm), into fragment **I**, exhibiting characteristic peaks in the aromatic (8.379(t), 7.964(d), 7.385, 7.363 and 7.152 ppm) and low-field benzylic (5.483, 5.224 and 5.007 ppm) regions, and two equivalents of **G1des(E)**, exhibiting aromatic signals at 8.348(t) and 7.863(d) (Scheme 3).[16] This transformation is completed in slightly over 24 h, so that after two days no traces of **G3des$_{1,3}$(E)** or of the fragment **H** (an intermediate between **G3des$_{1,3}$(E)** and **I**) are visible. The fragment **I** decomposes much more slowly into **G2des$_1$(OCOCF$_3$)** and two more equivalents of **G1des(E)**, in such a way that only after 2 weeks trace signals of the fragments **I** and **J** (an intermediate between **I** and **G2des$_1$(OCOCF$_3$)**) completely disappear from the spectrum. The dendron **G2des$_1$(OCOCF$_3$)**, the stable final product of the decomposition sequence, exhibits characteristic aromatic singlets at 7.333, 7.317 and 7.145 ppm as well as benzylic singlets at 5.474 and 4.980 ppm. The fragment **H**, being an intermediate between **G3des$_{1,3}$(E)** and **I**, is characterized by signals that are very close to those of the two fragments. However, even a slight difference (a few thousandth of ppm) results in a broadening of the combined peaks, when at least two of these three compounds are present. The same is true for the intermediate fragment **J** and the preceding and the succeeding compounds **I** and **G2des$_1$(OCOCF$_3$)**, respectively.

ES-MS measurements of the components of the cleavage solution fully support the aforementioned assignment and course of the events. Thus, in the solution analyzed with the positive ion detection mode *ca.* 45 minutes after the beginning of the cleavage, in the area above m/z = 800, $(M + Na)^+$ and $(M + K)^+$ peaks of **G3des$_{1,3}$(E)** (m/z 1385.5 and 1401.5 respectively) are the highest. The $(M + Na)^+$ peak of intermediate **H** (m/z 1289.5) is clearly visible, while a weak signal with m/z = 1193.4 points to a trace amount of compound **I**. Moreover in the negative ion detection mode $(M + CF_3CO_2)^-$ peaks of **G3des$_{1,3}$(E)**, **H** and **I** (m/z 1475.5, 1379.4 and 1283.4 respectively) are the highest in the area above m/z = 800. The ES-MS analysis of the cleavage mixture incubated for 24 hours exhibited the characteristic $(M + Na)^+$ and $(M + CF_3CO_2)^-$ peaks (in the positive and negative modes respectively) of **I, J** (m/z 1097.3 and 1187.3 respectively) and **G2des$_1$(OCOCF$_3$)** (m/z 1001.3 and 1091.3 respectively), without any signals of **H** or **G3des$_{1,3}$(E)**. After a seven day incubation, only the characteristic peaks of **G2des$_1$(OCOCF$_3$)** and **J** (trace amount) were visible.

We can now reconsider the factors that are responsible for the acidolytic disassembly of the two third-generation dendrons, and their "daughter" fragments. First, the current results support the conclusion of the previous study that the main factor leading to the observed acid-induced degradation of the dendrons is the weakening of the benzylic C–O bond, caused by the electron donating effect of the two alkyl substi-

tuents on the aromatic ring positioned *ortho* and *para* to this benzylic position. In the "hetero-dendron", the corresponding bonds of the module that lacks these substituents were not cleaved by the acid.

Another substituent that apparently affects the benzylic C–O bond lability and, through it, the rate of the dendrons' disassembly, is the *meta*-positioned hydroxy/benzyloxy group. While both **A** and **G2(E)** are presumably generated by the same event (Scheme 2), and **A**, contrary to **G2(E)**, cannot be generated by an alternative route, the decomposition of **G2(E)** occurs notably faster than that of the fragment **A**. Furthermore, the decomposition of the "hetero-dendron" **G2des$_2$(E)** in a 1 : 1 $CDCl_3$–TFA solution, described in our previous report,[7] is notably faster than the conversion of **G3des$_{1,3}$(E)** into **H**, or of **H** into **I**. In both cases a cleavage of the benzylic C–O bond takes place in a very similar environment with the only apparent disparity, to which the differences in the cleavage rates can be attributed, being the *meta*-to-benzyl substituent. It seems that the hydroxyl substituent affects faster cleavage, as compared to benzyloxy functionality.

It is clear now that, beyond the aforementioned electronic factors, the steric strain plays an important role in facilitating the disassembly in the described dendritic systems. Already in the previous report it was observed that **G2(E)** decomposes much faster than **D**, its successor in the disassembly chain, and similarly **G2des$_2$(E)** decomposes significantly faster than its "daughter" fragment **K** (Scheme 4).[7] In the current study, monitoring of the **G3(E)** demonstrated that, while **G3(E)** decomposes rapidly and disappears from the decomposition solution within 11 hours, its immediate successor **A**, which is generated in the mixture in a significant amount in the first few hours of the monitoring, decays significantly slower remaining in a countable amount in the mixture even after almost 2 days. Furthermore, while it takes slightly more than 24 hours for **G3des$_{1,3}$(E)** to be degraded, mostly to **I**, in the 1 : 1 $CDCl_3$–TFA cleavage solution, the monitoring demonstrates that only after 2 weeks **I** is fully degraded into **G2des$_1$(OCOCF$_3$)**. For all four pairs of compounds described above, the differences in the rates of decomposition, which proceeds through benzylic C–O bond cleavage, cannot be traced to the electronic influence of the presence or absence of the second dendritic arm. Such an influence will have to propagate through five bonds and this is highly unlikely. On the other hand, all full dendrons within the four pairs are more sterically crowded and, therefore, are likely to sustain a much stronger steric strain. This must be the reason for their significantly higher decomposition rate, as compared to their "one-arm" counterparts within the pair.

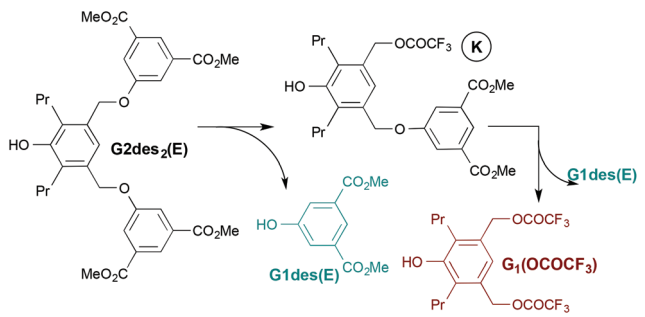

Scheme 4 The disassembly of the "hetero-dendron" **G2des$_2$(E)**.

Experimental

The third-generation dendrons were prepared on a Wang Bromo polystyrene resin (1% crosslinked divinylbenzene–styrene copolymer, 100–200 mesh, loading 0.90 mmol g^{-1}, Novabaiochem) according to the previously reported procedures.[7,9] ^{1}H NMR monitoring measurements were carried out on a Bruker AVANCE-400 spectrometer, in $CDCl_3$–TFA 9 : 1 or $CDCl_3$–TFA 1 : 1, with residual $CHCl_3$ (7.26 ppm), as calibration standard, and with benzene (7.36 ppm) or 1,1,2,2-tetrachloroethane (5.95 ppm), as internal standards. For these measurements, the resin was incubated with the cleavage solution for 30 min, filtered off, and the filtrate used for monitoring.

For the MS analysis, following the cleavage of the dendrons by $CDCl_3$–TFA solution (9 : 1, v/v for **G3(E)** and 1 : 1, v/v for **G3des$_{1,3}$(E)**), the resins were filtered off. At the designated times the solvents were evaporated. In order to ensure the complete evaporation of TFA, a small volume of ethyl acetate was added, the sample redissolved, and then the solvent was evaporated once again. This step was repeated 3 times. The MS spectra were recorded on a Waters Synapt-HDMS instrument.

Conclusions

Although the propyl substituents can impart both electronic and steric effects, sometimes inseparable, on the chemical behavior of organic molecules, in the case of the oligoether dendrons described in this work we have been able to analyze these factors separately by monitoring the dendron disassembly and comparing the rates of "decay" of parent dendrons and their fragments. Nevertheless, this analysis proved that both the electron donation and the steric strain induced by the propyls contribute in a synergistic way to the disassembly phenomenon. Importantly, it was demonstrated, for the first time, that steric strain significantly accelerates decomposition of a single dendron to its building modules.

Acknowledgements

This research was supported by grant no. 955/10 from the Israel Science Foundation and grant no. 2012193 from the United States–Israel Binational Science Foundation (BSF).

Notes and references

1 H. C. Brown and R. S. Fletcher, *J. Am. Chem. Soc.*, 1949, **71**, 1845–1854.

2 (*a*) *Dendrimers and other dendritic polymers*, ed. J. M. J. Fréchet and D. A. Tomalia, John Wiley & Sons, Chichester, 2001; (*b*) G. R. Newkome, C. N. Moorfield and F. Vögtle, *Dendrimers and dendrons. Concepts, synthesis, applications*, Wiley-VCH, Weinheim, 2001.
3 D. Ruiz-Molina, J. Veciana, F. Palacio and C. Rovira, *J. Org. Chem.*, 1997, **62**, 9009–9017.
4 (*a*) J.-S. Lee, J. Huh, C.-H. Ahn, M. Lee and T. G. Park, *Macromol. Rapid Commun.*, 2006, **27**, 1608–1614; (*b*) T. Etrych, L. Kovar, J. Strohalm, P. Chytil, B. Rihova and K. Ulbrich, *J. Controlled Release*, 2011, **154**, 241–248; (*c*) T. Etrych, J. Strohalm, P. Chytil, P. Cernoch, L. Starovoytova, M. Pechar and K. Ulbrich, *Eur. J. Pharm. Sci.*, 2011, **42**, 527–539.
5 (*a*) H. Yu, A. D. Schluter and B. Z. Zhang, *Helv. Chim. Acta*, 2012, **95**, 2399–2410; (*b*) G. Sanclimens, L. Crespo, M. Pons, E. Giralt, F. Albericio and M. Royo, *Tetrahedron Lett.*, 2003, **44**, 1751–1754.
6 (*a*) J. F. G. A. Jansen, E. M. M. de Brabander-van den Berg and E. W. Meijer, *Science*, 1994, **266**, 1226–1229; (*b*) P. Gandhi, B. Huang, J. C. Gallucci and J. R. Parquette, *Org. Lett.*, 2001, **3**, 3129–3132; (*c*) A. Kowalewska and W. A. Stańczyk, *ARKIVOC*, 2006, **5**, 110–115; (*d*) K. Chiad, M. Grill, M. Baumgarten, M. Klappez and K. Müllen, *Macromolecules*, 2013, **46**, 3554–3560.
7 J. Karabline and M. Portnoy, *Org. Biomol. Chem.*, 2012, **10**, 4788–4794.
8 For reviews on polyether dendrons, see: (*a*) S. M. Grayson and J. M. J. Frechet, *Chem. Rev.*, 2001, **101**, 3819–3867; (*b*) J. G. Li, C. Meng, X. Q. Zhang, L. Zhang and A. F. Zhang, *Prog. Chem.*, 2006, **18**, 1157–1180.
9 For synthesis of related less crowded dendrons on solid support, see: (*a*) A. Dahan and M. Portnoy, *Macromolecules*, 2003, **36**, 1034–1038; (*b*) A. Mansour, T. Kehat and M. Portnoy, *Org. Biomol. Chem.*, 2008, **6**, 3382–3387.
10 For brevity only the aromatic region is shown. For the area of low-field benzylic signals, see ESI.†
11 B. Helms, C. O. Liang, C. J. Hawker and J. M. J. Fréchet, *Macromolecules*, 2005, **38**, 5411–5415.
12 Low field signals of the *O*-substituted benzylic positions were used for the characterization of the mixture components, while the high-field benzylic signals of the propyl substituents were not.
13 Fragments with lower molecular mass seem to have lower affinity toward the trifluoroacetate anion and, hence, exhibit smaller peaks, or do not exhibit peaks at all, in the negative ion detection mode.
14 The low molecular masses of **G1(E)** and **G1(OCOCF$_3$)**, both of which must be present in the reaction mixture, is the likely reason for the absence of their $(M + Na)^+$, $(M + CF_3CO_2)^-$ or $(M - H)^-$ peaks in the spectra.
15 des stands for des-dipropyl, while $des_{1,3}$ indicates that this third-generation dendron lacks propyl substituents on the first and third layer modules; for spectra see ESI.†
16 A minor gradual change in the chemical shifts of the fragment signals was observed over the 2 weeks, due to the slow evaporation of $CDCl_3$ from the cleavage mixture. In order to compensate, small amount of $CDCl_3$ was added before the 14th day measurement, leading to an opposite shift. Accordingly, chemical shifts reported in the manuscript are those observed within the first 2 days of monitoring.

